JOURNAL OF MATERIALS SCIENCE **38** (2003) 3775–3782

Sintering behavior of Ni/Y_2O_3-ZrO_2 cermet electrodes of solid oxide fuel cells

SAN PING JIANG
Fuel Cells Strategic Research Program, School of Mechanical and Production Engineering, Nanyang Technological University, Singapore 639798
E-mail: mspjiang@ntu.edu.sg

The sintering behavior of Ni/Y_2O_3-ZrO_2 (YSZ) cermet electrode coating on 3 mol% Y_2O_3-ZrO_2 electrolyte was studied under moist and dry hydrogen atmosphere at 1000°C for up to 2000 h. The sintering behavior of Ni/YSZ cermet electrodes was dominated by the agglomeration and grain growth of Ni particles in the cermets, which was critically related to the content of Ni and YSZ phases in the cermet. For pure Ni electrode coating, the sintering was substantial and cross plane cracks and isolated Ni island were formed after sintering at 1000°C for only 250 h. However with the addition of YSZ phase, the sintering of Ni/YSZ cermet anode coatings was significantly reduced. For the cermet composition of Ni (50 vol%)/YSZ (50 vol%), the change in the surface porosity and pore size distribution after sintering at 1000°C for 2000 h was very small. The microstructural stability of the Ni (50 vol%)/YSZ (50 vol%) cermet electrodes was also demonstrated by the performance stability tested under current load of 250 $mAcm^{-2}$ at 1000°C for over 2500 h.

1. Introduction

In solid oxide fuel cells, the stability and sintering behavior of electrode materials such as Sr-doped $LaMnO_3$ (LSM) cathode and Ni/Y_2O_3-ZrO_2 (Ni/YSZ) cermet anode is a major concern for the long-term performance during fuel cell operation at high temperatures [1–10]. This is particular true for the Ni/YSZ cermet electrodes due to the non-wettability between metallic Ni and ceramic YSZ (the contact angel is 117° at 1500°C) [11]. Iwata [1] showed that Ni particles in the Ni/YSZ cermets grew significantly from initial particle size of less than 1 μm to 10 μm under fuel cell operation conditions of 0.3 Acm^{-2} for only 1015 h at 1000°C and the agglomeration of Ni particles led to the significant reduction in the three phase boundary areas and the increase in the electrode polarization resistance. By proper combination of coarse and fine YSZ particles in the cermets, Itoh *et al.* [12] showed that the performance stability of the Ni/YSZ cermet anodes was improved substantially. Optimization of phase distribution between Ni and YSZ was found to be critical in the inhibition of agglomeration and sintering of the Ni particles in particular and to improve the performance stability of SOFC [13]. Simwonis *et al.* [14] recently studied the effect of Ni sintering on the electronic conductivity and microstructure of Ni/8 mol% Y_2O_3-ZrO_2 cermet substrates at 1000°C for 4000 h. The results clearly show that the microstructural change of Ni/YSZ cermet substrate is mainly due to the sintering and agglomeration of Ni particles while the changes in the YSZ particle and porosity distribution are very small. The agglomeration of Ni particles led to a decrease of the electronic conductivity of the cermet substrates. This is due to the fact that the conductivity of Ni/YSZ cermets is dependent on the microstructure and distribution of Ni and YSZ particles [15, 16]. However, there is generally lack of information of the sintering behavior and microstructural change of Ni/YSZ cermet electrode coatings under SOFC operation conditions. This is largely related to the practical difficulty in the monitoring of the microstructure change of the electrode coating during fuel cell operation. Nevertheless, the information on the sintering behavior of Ni/YSZ cermet electrode coatings is important for understanding of the long-term performance behavior of SOFC. In this paper, we report the investigation of the morphological change and sintering behavior of Ni/YSZ cermet electrode coatings as a function of the cermet composition and sintering conditions at 1000°C. The relationship between the microstructure, sintering behavior and Ni/YSZ cermet composition is discussed.

2. Experimental

The zirconia electrolyte substrates were prepared from 3 mol% Y_2O_3–ZrO_2 (TZ3Y, Tosoh, Japan) by tape casting and sintering at 1500°C. NiO (Ajax, Australia) and TZ3Y were thoroughly mixed by ball milling and the cermet ink was applied to TZ3Y substrates by screen-printing, followed by sintering at 1400°C for 2 h in air. Three different anodes were prepared with compositions of 100% Ni (Ni), Ni (70 vol%)/TZ3Y (30 vol%) and Ni (50 vol%)/TZ3Y (50 vol%). The electrode coating thickness was ~50 μm and the electrode area was 0.442 cm^2.

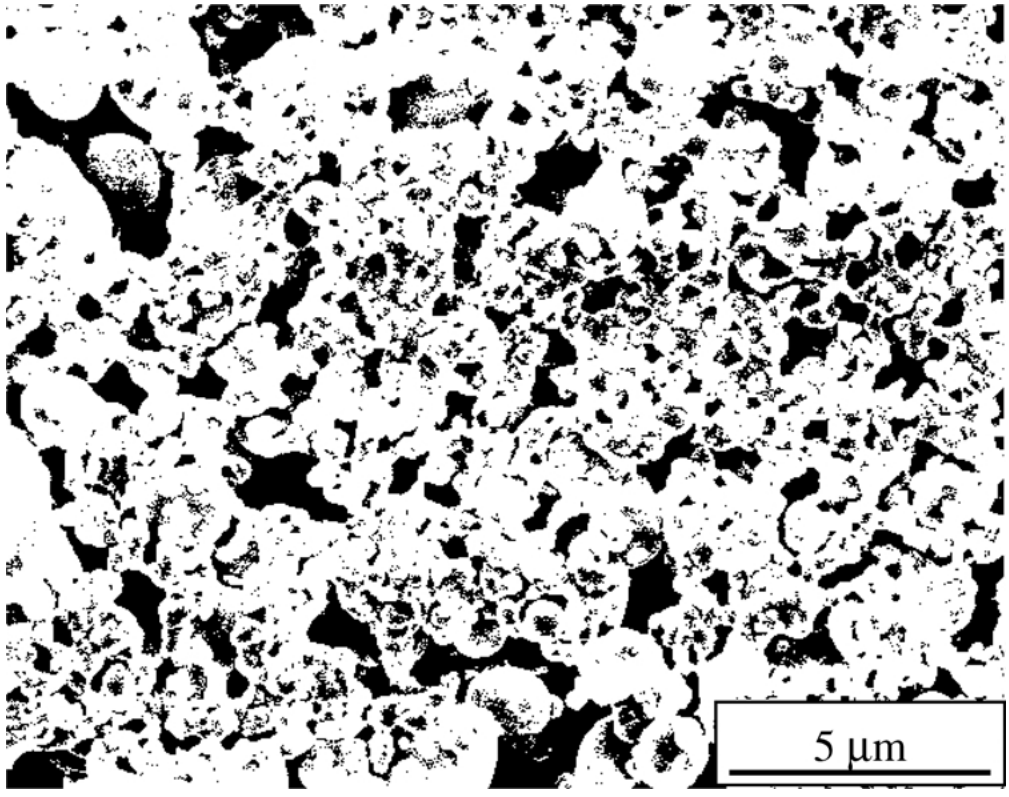

Figure 1 Typical binary image from a SEM image of a Ni (50 vol%)/TZ3Y (50 vol%) cermet electrode coating.

Sintering of the electrode coating sample was carried out in a close-end alumina tube under reducing atmosphere of 10%H_2/90%N_2 humidified at room temperature through a water bubbler (H_2O content in the fuel gas was ∼3%, referred to moist 10%H_2/90%N_2). The electrode coating samples were placed on an alumina boat inside the close-end tube and heated to 1000°C. The samples were taken out after sintering for certain period (1 h, 250 h, 750 h, and 2000 h). After image analysis, the samples were put back into the furnace for further sintering. The heating and cooling rate was 300°C/h and hydrogen was passing through the sample during the heating and cooling to avoid an oxidation of the sample. In comparison, sintering of the electrode coating samples was also carried out under reducing atmosphere of 10%H_2/90%N_2 without humidification (referred to dry 10%H_2/90%N_2) at 1000°C for 750 h.

Scanning electron microscopy (SEM) was used for the image analysis. The SEM images of the surface morphology of the coating were analyzed using the "Prism View" software. The computer program defines the porous area of the image as black in color whereas the Ni and TZ3Y particles as white. In doing so, a binary image of the porous structure is obtained. Fig. 1 shows typical binary image of a SEM picture of a Ni (50 vol%)/TZ3Y (50 vol%) cermet coating. The overall porosity of the image was 23.7%. However, the image analysis produced by the "Prism View" program only gave the total surface porosity, not the porosity distribution. In order to obtain the information of porosity distribution, the binary image was produced and mapped with scaled transparence paper and area of the individual pores were manually counted. The manual counting was a tedious process. However, it did have an advantage of better assessment of actual pores from false ones. The diameter of the pores was calculated based on normalized circular area. It should be pointed here that circular area is a crude approximation to the real situation as most pores are not circular as shown in Fig. 1. The image analysis was generally taken as 5 K magnification and five images were randomly taken in different areas of the coating surface. The actual surface area covered by each SEM image was approximately 2.8×10^{-4} mm^2 and the total surface area analyzed was 1.4×10^{-3} mm^2. Each square in the grid paper was 4 mm^2 and the actual area covered by each square in the case of 5 K magnification SEM images was 0.032 μm^2. Thus the minimum diameter of pores which can be measured was 0.2 μm. The relative frequency of occurrence of pores was plotted against the normalized pore diameter, thus giving the information on the porosity distribution as a function of anode cermet composition and sintering time. The average grain size of Ni and TZ3Y particles was also measured by using scaled transparence paper directly on SEM images.

An electrochemical stability test was also carried out on a cell with Ni (50 vol%)/TZ3Y (50 vol%) cermet anode and $La_{0.72}Sr_{0.18}MnO_3$ (LSM) cathode at 1000°C under a constant current of 250 $mAcm^{-2}$ for 2543 h. In this case, 50 mm × 50 mm TZ3Y electrolyte cell was used and the electrolyte thickness was 194 μm. Ni/TZ3Y cermet anode and LSM cathode were applied to TZ3Y electrolyte by screenprinting, followed by sintering at 1400°C and 1150°C, separately. The electrode surface area was 13 cm^2. The fuel composition at the anode side was 96%H_2/4%H_2O and air was used as the oxidant gas. The flow rate of the H_2 fuel and air was 1000 sccm. Pt mesh was used as current collector on the cathode and Ni mesh on the anode. Fuel and air were directed on to the center of the electrode surface

and distributed evenly across the electrode area through distribution channels of alumina manifolds. The cell configuration was similar to that given elsewhere [17].

3. Results and discussion

The SEM pictures of Ni, Ni (70 vol%)/TZ3Y (30 vol%) and Ni (50 vol%)/TZ3Y (50 vol%) cermet electrode coatings before reduction and after reduction in situ and sintering under moist 10%H_2/N_2 at 1000°C for 1 h, 250 h, 750 h and 2000 h are shown in Figs 2 and 3. The observations are as follows.

Before the reduction process, Ni existed as NiO in the cermets and showed distinct NiO crystalline facets (Fig. 2a1). For pure Ni anode, the grain size of NiO was in the range of 4.3 μm to 0.9 μm and the average grain size was 2.24 ± 0.99 μm. For both Ni (70 vol%)/TZ3Y (30 vol%) and Ni (50 vol%)/TZ3Y (50 vol%) samples TZ3Y particles were distributed among NiO particles. The average particles size of NiO was 1.12 ± 0.25 μm and was similar for both Ni (70 vol%)/TZ3Y (30 vol%) and Ni (50 vol%)/TZ3Y (50 vol%) cermets. The particle size of NiO in the Ni/TZ3Y cermets was clearly smaller as compared with that for pure Ni anode, indicating that zirconia particles in the cermet inhibited the sintering of NiO particles. Transgranular cracks were also seen to occur at the top layer of the electrode coating. This may be due to the differences between the thermal expansion coefficient between the NiO and TZ3Y electrolyte substrate as the transgranular cracks were observed for both NiO/TZ3Y and NiO coatings.

After the samples were reduced and sintered in moist 10%H_2/N_2 at 1000°C for 1 h, the formation of continuous Ni-to-Ni network was seen for pure Ni anode coating (Fig. 2a2). For Ni/TZ3Y cermet anodes, continuous Ni-to-Ni network with Ni particles surrounded by fine TZ3T particles was also observed (Fig. 2b2 and c2). There is an increase of the Ni particle size despite the fact of the volume reduction of ~25% after reducing NiO to metallic Ni. The average particle size of Ni was 1.57 ± 0.49 μm for Ni (70 vol%)/TZ3Y (30 vol%) and 1.50 ± 0.55 μm for Ni (50 vol%)/TZ3Y (50 vol%) cermets, higher than that before the reduction (1.12 ± 0.25 μm). This indicates

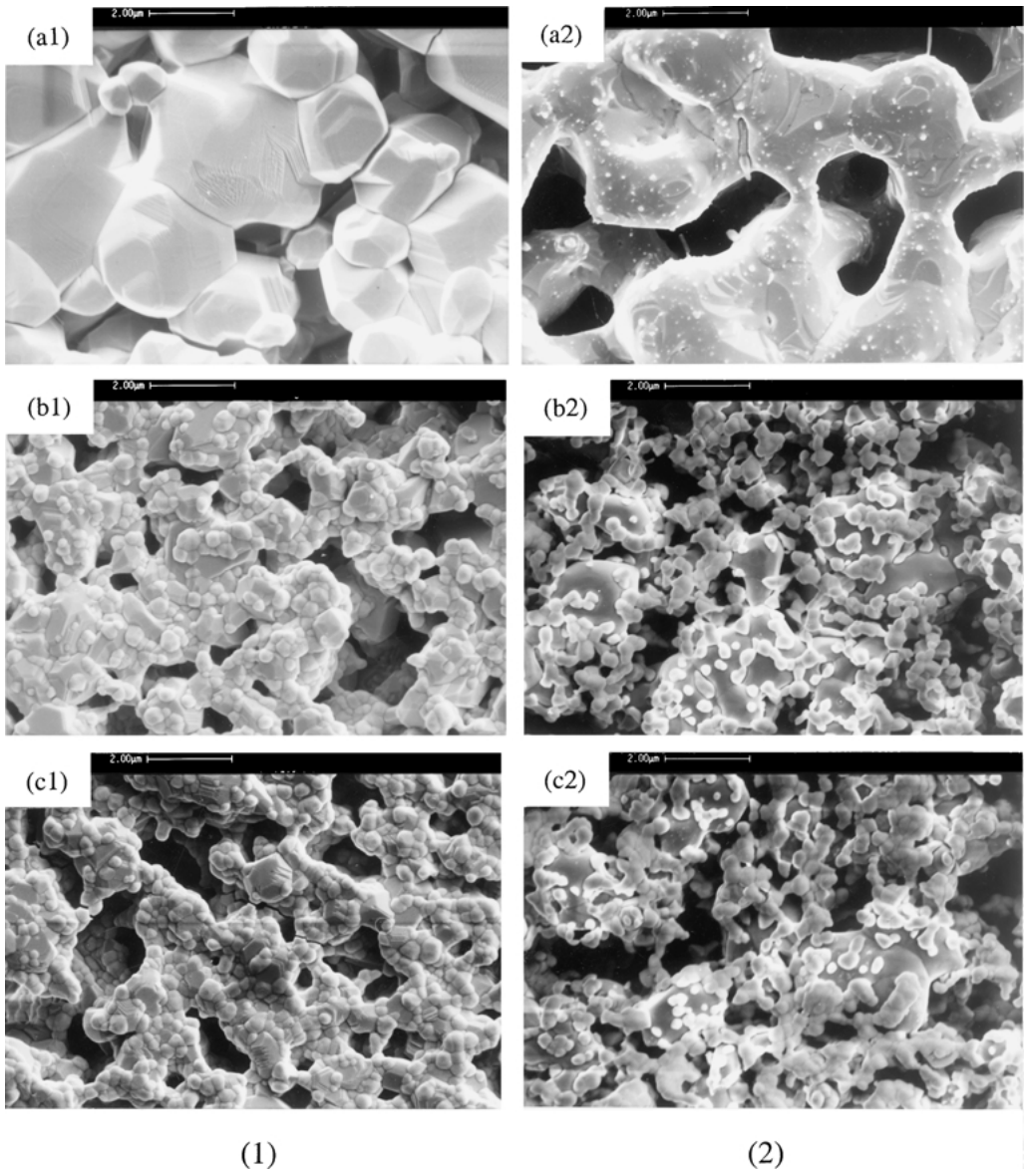

Figure 2 SEM pictures of (a) Ni, (b) Ni (70 vol%)/TZ3Y (30 vol%) and (c) Ni (50 vol%)/TZ3Y (50 vol%) before reduction (1) and after reduction and sintering under moist 10%H_2/90%N_2 at 1000°C for 1 h (2).

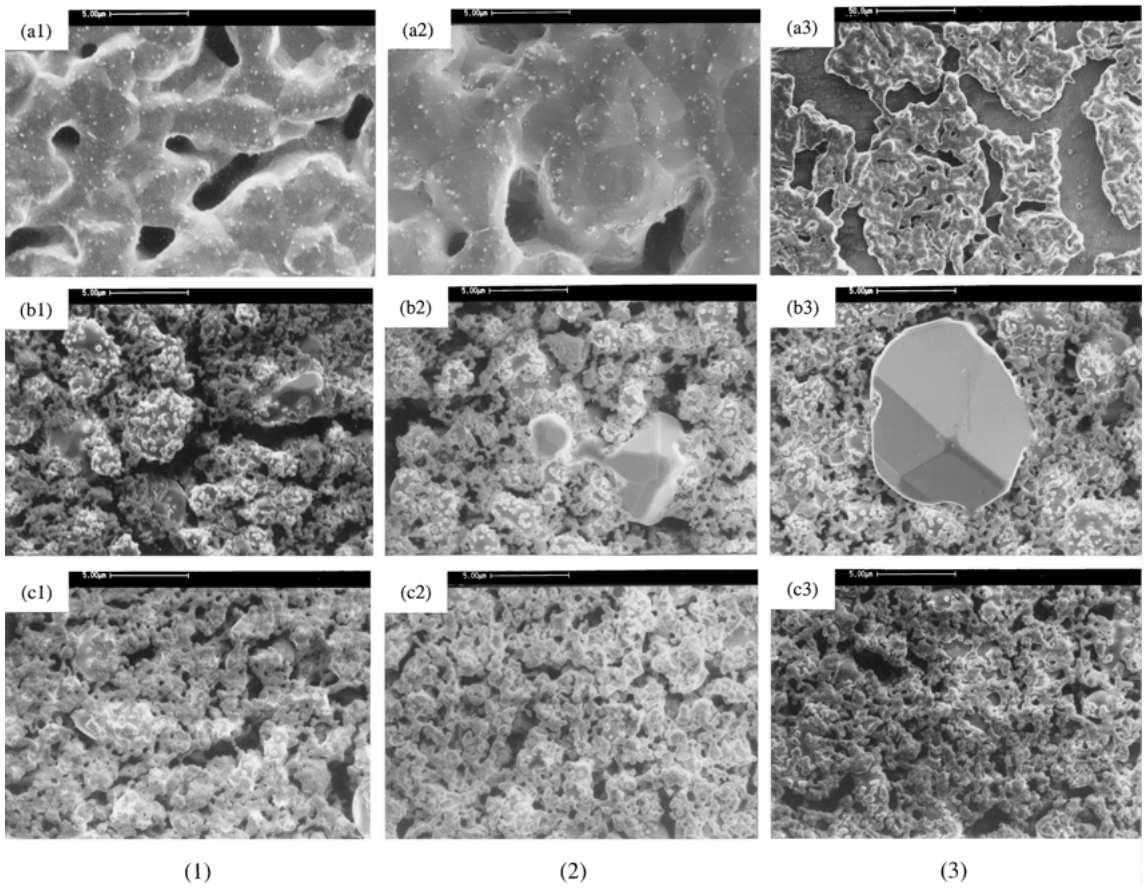

Figure 3 SEM pictures of (a) Ni, (b) Ni (70 vol%)/TZ3Y (30 vol%) and (c) Ni (50 vol%)/TZ3Y (50 vol%) after sintering under moist 10%H_2/90%N_2 at 1000°C for 250 h (1), 750 h (2) and 2000 h (3).

the strong tendency of the agglomeration and growth of fine Ni particles when NiO is reduced to metallic Ni under reducing atmosphere of moist hydrogen. The volume reduction and agglomeration of Ni phase in the cermet under fuel reducing environment would lead to the increase in porosity and the decrease in three phase boundaries [18]. The porous structure of Ni/TZ3Y cermet anode was characterized by fine TZ3Y deposited on relatively large Ni particles. At the same time, a continuous YSZ-to-YSZ network appears to be formed. One interesting feature to note here is that the transgranular cracks observed for samples prior to the reduction process is no longer detected after the reduction process, and no significant cracks were observed on the anode coating surface as well.

However, when the sintering time was increased to 250 h and 750 h, some changes in the microstructure were noted. A prolonged sintering caused the agglomeration and grain growth of Ni particles. For pure Ni anodes, the change in the morphology of electrode coating was dramatic. Sintering at 1000°C for 250 h caused the formation of cracked structure, characterized by isolated islands with gaps between the island blocks as large as 10 μm (see following sections). This is most likely related to the significant shrinkage and contraction of the Ni coating due to the rapid agglomeration and grain growth of Ni particle. For Ni/TZ3Y cermet anodes, the change in microstructure was much slower. However, the change in morphology depended on the Ni and YSZ contents in the cermet. For the cermet with 70 vol% Ni, the change in the surface morphology is more obvious and visible as compared to that with lower Ni content such as Ni (50 vol%)/TZ3Y (50 vol%). For Ni (70 vol%)/TZ3Y (30 vol%) cermet electrode coating, bright Ni particles were observed to grow outward after sintering at 1000°C for 250 h and the Ni particles became bigger after sintering for 750 h (Fig. 3b1 and b2). On the other hand, for Ni (50 vol%)/TZ3Y (50 vol%) cermet coating there was no clear observation of outward growth of Ni particles and almost no change in the morphology of the electrode coating (Fig. 3c1 and c2). As sintering time increased to 2000 h, Ni crystal growth and crack formation and propagation for the Ni (70 vol%)/TZ3Y (30 vol%) cermet electrode coating became worse. The size of the Ni crystal grown outward of the surface was as large as 11 μm in diameter (Fig. 3b3). On the other hand the outward growth of Ni crystals was not significant for the cermet samples of Ni (50 vol%)/TZ3Y (50 vol%) (Fig. 3c3), indicating that sintering behavior of Ni/YSZ cermet anodes is strongly dependent on the Ni and YSZ content in the cermet.

Fig. 4 shows the surface morphology of electrode coatings before and after sintered at 1000°C for up to 2000 h in moist 10%H_2/90%N_2. Before the sintering the quality of cermet electrode coating produced by screenprinting was similar for both Ni and Ni/TZ3Y cermets. The coating was characterized by smooth surface with occasional pinholes and small isolated cracks (Fig. 4a). Fore pure Ni coating, cracking was particularly significant and grown into isolated islands after sintering for only 250 h (Fig. 4b). After sintered at 1000°C for 2000 h, long cracks were

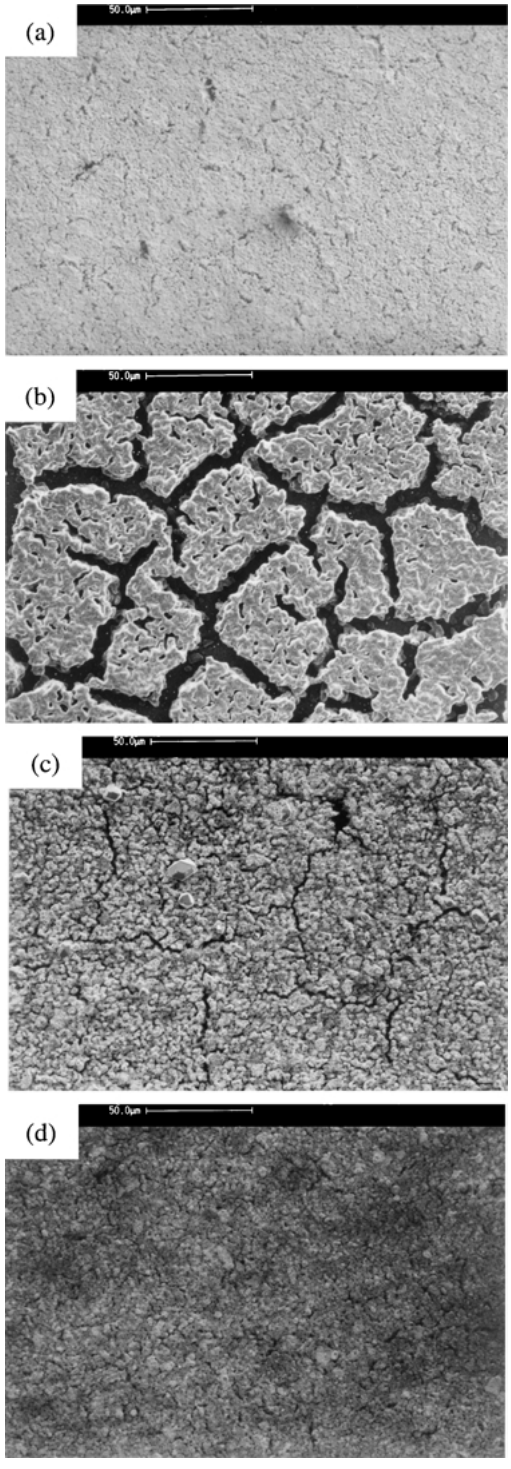

Figure 4 Surface pictures of (a) Ni electrode coating before the sintering, (b) Ni electrode coating after sintering for 250 h, (c) Ni (70 vol%)/TZ3Y (30 vol%) coating after sintering for 2000 h and (d) Ni (50 vol%)/TZ3Y (50 vol%) after sintering for 2000 h at 1000°C in moist $10\%H_2/90\%N_2$.

gradually developed on the surface of Ni (70 vol%)/TZ3Y (30 vol%) cermet electrode coating (Fig. 4c). In the case of Ni (50 vol%)/TZ3Y (50 vol%) cermet electrode, the number of long cracks on the coating surface were clearly much smaller as compared to that on the Ni (70 vol%)/TZ3Y (30 vol%) cermet electrode coating (Fig. 4d). The crack development is most likely related to the outward growth of Ni particles as observed on Ni (70 vol%)/TZ3Y (30 vol%) cermet electrode coatings (Fig. 3b).

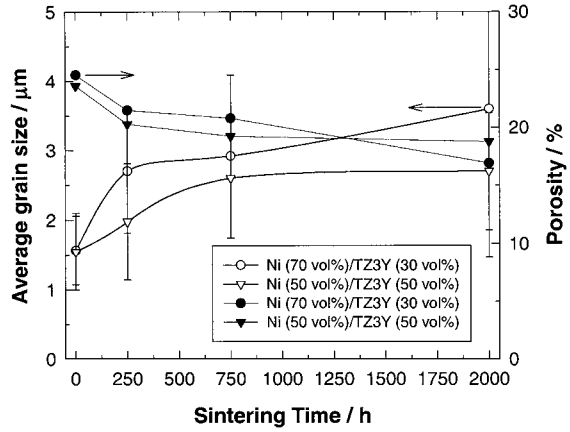

Figure 5 Average particle size of Ni phase in the cermet (open symbols) and porosity (close symbols) as a function of sintering time under moist $10\%H_2/90\%N_2$ at 1000°C.

The particle size measurements from SEM image analysis have revealed no significant growth of TZ3Y particle and no significant change in the distribution of TZ3Y phase. The average particle size of TZ3Y particles was 0.32 ± 0.12 μm for both cermet compositions and remained unchanged over the sintering period of 2000 h. However, the porosity and grain growth of Ni particles were related to the cermet composition. Fig. 5 shows the plot of average particle size of Ni phase in the cermet and porosity of the cermet as a function of sintering time at 1000°C. The initial particle size of Ni phase was 1.54 ± 0.55 μm, similar for both Ni (70 vol%)/TZ3Y (30 vol%) and Ni (50 vol%)/TZ3Y (50 vol%) cermet coatings. After sintering at 1000°C for 2000 h, average size of Ni particles in the cermet increased to 3.60 ± 2.13 μm for Ni (70 vol%)/TZ3Y (30 vol%) and 2.7 ± 0.84 μm for Ni (50 vol%)/TZ3Y (50 vol%), respectively. The agglomeration and grain growth of Ni particles of Ni (70 vol%)/TZ3Y (30 vol%) cermet electrodes were higher than that of Ni (50 vol%)/TZ3Y (50 vol%) cermet electrodes. The sintering profile of these two cermet electrode coatings also appears to be different. In the case of Ni (70 vol%)/TZ3Y (30 vol%) cermet coating, Ni particles grew relatively fast in the first 250 h and continuously grew at a slower rate. For Ni (50 vol%)/TZ3Y (50 vol%) cermet coating, Ni particles grew initially and the agglomeration and grain growth were much smaller after sintering for 750 h, reaching a plateau.

In general, there is a decrease of the overall porosity with the sintering time (Fig. 5). The initial porosity of the Ni/TZ3Y cermet coatings was in the range of ~25%. After sintered at 1000°C for 2000 h, porosity of Ni (70 vol%)/TZ3Y (30 vol%) decreased to ~17% while that of Ni (50 vol%)/TZ3Y (50 vol%) decreased to ~19%. The slightly high porosity of Ni (70 vol%)/TZ3Y (30 vol%) is most likely due to the high Ni content as compared to that of Ni (50 vol%)/TZ3Y (50 vol%) cermet coating. However, the change in the porosity is much slower for Ni (50 vol%)/TZ3Y (50 vol%) cermet as compared to that of Ni (70 vol%)/TZ3Y (30 vol%) cermet particularly after sintering for more than 250 h. The porosity results are consistent with the observed

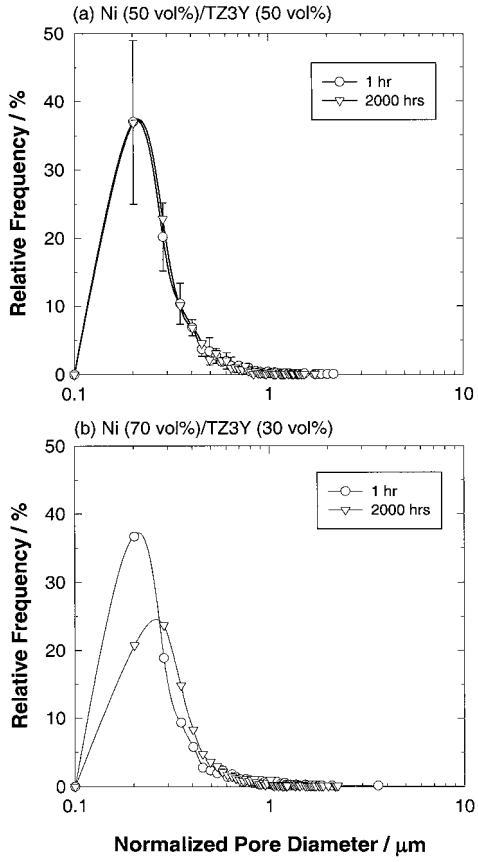

Figure 6 Pore size distribution of Ni (50 vol%)/TZ3Y (50 vol%) and Ni (70 vol%)/TZ3Y (30 vol%) cermet coatings sintered under moist $10\%H_2/90\%N_2$ atmosphere at 1000°C for 1 h and 2000 h.

microstructure and grain growth of Ni particles in the cermet coating. The trend of the decrease of the porosity of the Ni (50 vol%)/TZ3Y (50 vol%) cermet coating with sintering time is similar to that of the Ni (50 vol%)/YSZ (50 vol%) powder mixture prepared by mechanical alloying and sintered at 1350°C [10]. The porosity measured from the surface of electrode coating is generally lower than that measured from the bulk of the electrodes. Chou *et al.* [19] used filtration method with petroleum jelly to measure the porosity of the slurry-coated Ni/YSZ cermet coatings and found that porosity varied between 30% to 37%. From the cross-section of Ni/YSZ cermet substrate, the image analysis gave a porosity value of 37% [14]. The lower porosity measured from the coating surface may be related to the segregation and fast growth of Ni particles at the surface region. Nevertheless, the results of surface porosity distribution change are correlated very well with the agglomeration and grain growth of Ni particles and microstructural change of the Ni/TZ3Y cermet electrode coatings. The result confirms that sintering behavior of Ni/YSZ cermet electrode coatings is dominated by the kinetics of agglomeration and grain growth of Ni particles in the cermets [14].

Fig. 6 shows the pore size distribution of Ni (50 vol%)/TZ3Y (50 vol%) and Ni (70 vol%)/TZ3Y (30 vol%) cermet samples sintered under moist $10\%H_2/90\%N_2$ atmosphere for 1 h and 2000 h. To simplify the graph, the pore size distribution data for sintering at other sintering times were omitted. The pore size distribution for pure Ni sample was not measured as the severe cracking and agglomeration of Ni particles occurred with prolonged sintering as shown in Fig. 4. A typical example of standard deviation in the pore size measurement is given for the pore size distribution of a Ni (50 vol%)/TZ3Y (50 vol%) cermet sample sintered for 1 h. The error in the measurement of pore size distribution was high for small pores and became small as the pore size increased. For Ni (70 vol%)/TZ3Y (30 vol%) cermet coating, the pore size was shifted to coarser pores with reduced relative frequency after sintered for 2000 h. Again, for Ni (50 vol%)/TZ3Y (50 vol%) cermet coating, there was little change in the pore size distribution even after sintering for 2000 h. The same stability of porous structure was also observed for Ni (40 vol%)/YSZ (60 vol%) cermet substrates after sintered at 1000°C for 4000 h where the pore size distribution was measured from the cross-section of the cermet sample [14]. This indicates that the information obtained from the surface morphology is relevant to the microstructure change of the cermet electrode coatings.

The sintering atmosphere seems to have some effect on the agglomeration and grain growth of Ni particles in the cermets. Fig. 7 shows the SEM pictures of Ni, Ni (70 vol%)/TZ3Y (30 vol%) and Ni (50 vol%)/TZ3Y

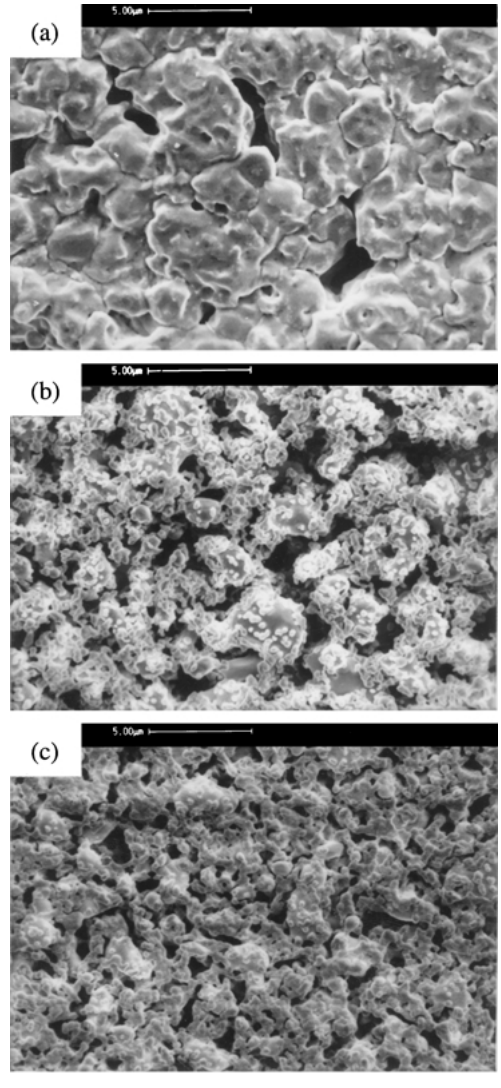

Figure 7 SEM pictures of (a) Ni, (b) Ni (70 vol%)/TZ3Y (30 vol%) and (c) Ni (50 vol%)/TZ3Y (50 vol%) after sintering under dry $10\%H_2/90\%N_2$ at 1000°C for 750 h.

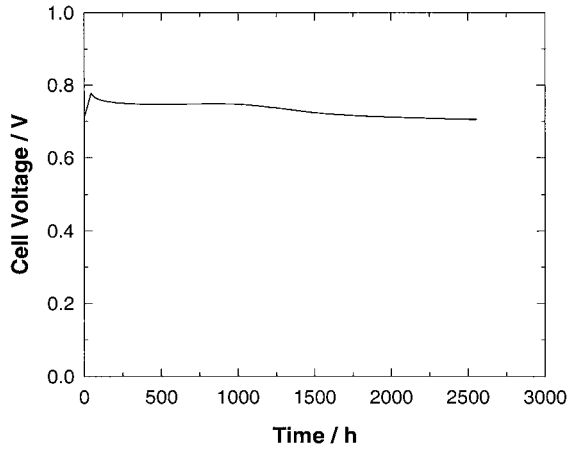

Figure 8 Cell performance of a 50 mm × 50 mm cell with Ni (50 vol%)/TZ3Y (50 vol%) anode and LSM cathode under current density of 250 $mAcm^{-2}$ and 96% H_2/4%H_2O at 1000°C.

(50 vol%) after sintering under dry 10%H_2/90%N_2 at 1000°C for 750 h. Compared to those sintered under moist 10%H_2/90%N_2 at 1000°C for the same period, the general appearance and porous structure of the cermet anode samples are similar. However, water appears to play some role in the Ni crystal agglomeration and growth process. The pure Ni sample behaved differently in the sintering process and the Ni particles were smaller in size in dry 10%H_2/90%N_2 as compared to that in moist 10%H_2/90%N_2 (see Figs 3a2 and 7a). No significant Ni crystal outward growth was observed in the sintering experiment in the dry 10%H_2/N_2 atmosphere for Ni (70 vol%)/TZ3Y (30 vol%) sample (Fig. 7b). This indicates that the surface diffusion coefficient of Ni atoms may be affected by the presence of water vapor as the surface diffusion of Ni is considered to be the dominant mechanism for the agglomeration and grain growth of Ni at high temperatures [14].

Fig. 8 shows the cell performance of a 50 mm × 50 mm cell with Ni (50 vol%)/TZ3Y (50 vol%) anode and LSM cathode under current density of 250 $mAcm^{-2}$ and 96%H_2/4%H_2O at 1000°C. Fig. 9 is the SEM picture of the Ni/TZ3Y cermet electrode coating after the testing. The relatively high open porosity of the coating was partly due to the fact that the anode was prepared by addition of graphite pore-formers, which in general increased the porosity of the coating by ∼10% [13]. The overall cell performance deterioration was 53 mV over 2543 h testing and this was corresponding to a polarization loss of 21 mV over 1000 h. The maximum cell voltage obtained was 0.759 V. Thus the drop of cell voltage was 2.7% per 1000 h. The overpotential values for the anode and cathode were not measured for this cell. Based on the evaluation of polarization performance of similar cells with reference electrodes tested for over 4000 h [13], the distribution of the cell polarization losses was 30% from the Ni/YSZ cermet anodes, 46% from LSM cathode and 24% from the TZ3Y electrolyte for the first 2000 h. This indicates that in solid oxide fuel cells based on Ni/YSZ cermet anodes and LSM cathodes, the polarization losses on the anode side are not dominating as compared to that on the cathode side. Nevertheless, optimization of the Ni and YSZ distribution in the Ni/YSZ cermet anodes can

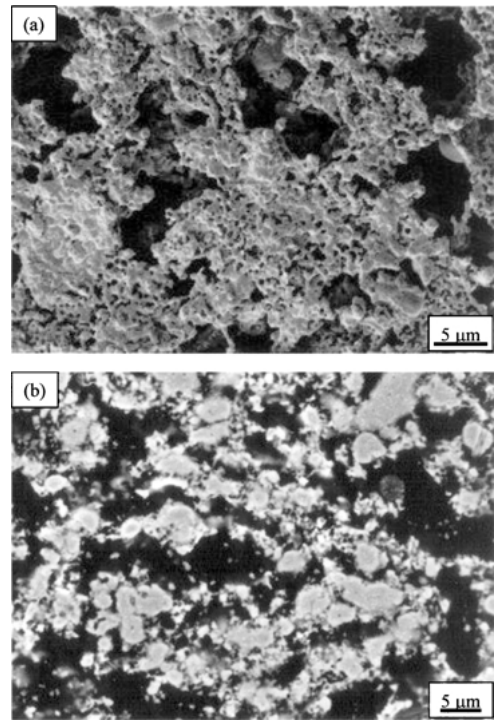

Figure 9 SEM pictures of the Ni (50 vol%)/TZ3Y (50 vol%) cermet anode of the cell in Fig. 8 after testing: (a) the surface and (b) the cross-section.

significantly reduce the agglomeration and grain growth of Ni particles in the cermet and thus enhance the microstructure and performance stability of the anodes, as indicated by the different sintering behavior of Ni, Ni (70 vol%)/TZ3Y (30 vol%) and Ni (50 vol%)/TZ3Y (50 vol%) cermet anodes in the present study.

4. Conclusions

The sintering behavior of Ni/YSZ cermet electrode coatings was dominated by the agglomeration and grain growth of Ni particles in the cermets. The Ni phase agglomeration and growth as well as crack formation and propagation of the electrode coating increased with the increase of Ni content in the Ni/zirconia cermets. For pure Ni electrode coating, the sintering was significant and cross plane cracks and isolated Ni islands were formed after sintering at 1000°C for only 250 h. Addition of YSZ phase in the cermet significantly reduced the sintering rate of Ni/YSZ cermet electrode coatings. The agglomeration and grain growth of Ni particles and the change in the porosity and pore size distribution of Ni/YSZ cermet anodes are strongly dependent on the distribution of Ni and YSZ phase, as demonstrated by the significant differences in the sintering behavior of Ni, Ni (70 vol%)/YSZ (30 vol%) and Ni (50 vol%)/YSZ (50 vol%) cermet electrode coating.

Water is believed to play some role in the promotion of the Ni particle agglomeration and growth.

Acknowledgement

I would like to thank Dr Ken Lai for his assistance in the image analysis and Dr Y. Ramprakash for the cell performance testing.

References

1. T. IWATA, *J. Electrochem. Soc*. **143** (1996) 1521.
2. H. ITOH, T. YAMAMOTO, M. MORI and T. ABE, in "SOFC IV," edited by M. Dokiya, O. Yamamoto, H. Tagawa and S. C. Singhal (The Electrochemical Society, Pennington, NJ, 1995) p. 639.
3. D. HERBSTRITT, A. WEBER and E. IVERS-TIFFÉE, in "SOFC VI," edited by S. C. Singhal and M. Dokiya (The Electrochemical Society, Pennington, NJ, 1999) p. 972.
4. M. J. JÖRGENSEN, P. HOLTAPPELS and C. C. APPEL, *J. Appl. Electrochem*. **30** (2000) 411.
5. S. P. JIANG, J. P. ZHANG, Y. RAMPRAKASH, D. MILOSEVIC and K. WILSHIER, *J. Mater. Sci.* **35** (2000) 2735.
6. A. KHANDKAR, S. ELANGOVAN and M. LIU, *Solid State Ionics* **52** (1992) 57.
7. A. IOSELEVICH, A. A. KORNYSHEV and W. LEHNERT, *J. Electrochem. Soc*. **144** (1997) 3010.
8. R. VAßEN, D. SIMWONIS and D. STÖVER, *J. Mater. Sci*. **36** (2001) 147.
9. S. P. S. BADWAL, *Solid State Ionics* **143** (2001) 39.
10. R. WILKENHOENER, R. VAßEN, H.P. BUCHKREMER and D. STÖVER, *J. Mater. Sci*. **34** (1999) 257.
11. A. TSOGA, A. NAOMIDIS and P. NIKOLOPOULOS, *Acta Mater.* **44** (1996) 3679.
12. H. ITOH, T. YAMAMOTO, M. MORI, T. HORITA, N. SAKAI, H. YOKOKAWA and M. DOKIYA, *J. Electrochem. Soc*. **144** (1997) 641.
13. S. P. JIANG, P. J. CALLUS and S. P. S. BADWAL, *Solid State Ionics* **132** (2000) 1.
14. D. SIMWONIS, F. TIETZ and D. STÖVER, *ibid.* **132** (2000) 241.
15. W. HUEBNER, D. M. REED and H. U. ANDERSON, in "SOFC-VI," edited by S. C. Singhal and M. Dokiya (The Electrochemical Society, Pennington, NJ, 1999) p. 503.
16. Y. M. PARK and G. M. CHOI, *Solid State Ionics* **120** (1999) 265.
17. S. P. JIANG, J. G. LOVE and Y. RAMPRAKASH, *J. Power Sources* **110** (2002) 201.
18. S. P. JIANG, Y. Y. DUAN and J. G. LOVE, *J. Electrochem. Soc.* **149** (2002) A1175.
19. K. C. CHOU, S. YUAN and U. PAL, in "SOFC III," edited by S. C. Singhal and H. Iwahara (The Electrochemical Society, Pennington, NJ, 1993) p. 431.

Received 18 November 2002
and accepted 7 July 2003